n-type silicon pad array detector test at PS, CERN

Sawan, G. J. Tambave, K. P. Sharma, M. Mondal, L. Kumar, R. Singh, B. Mohanty

ALICE-STAR India Collaboration Meeting

23rd November, 2023

Outline

- Test setup
- Noise estimation
- Response to pion beam
  - MIP signal
  - Detector operating voltage scan
  - Gain correction
- Response to electron beam
  - Longitudinal shower profile
  - Transverse energy profile
- Summary

Tests beam setup at PS CERN

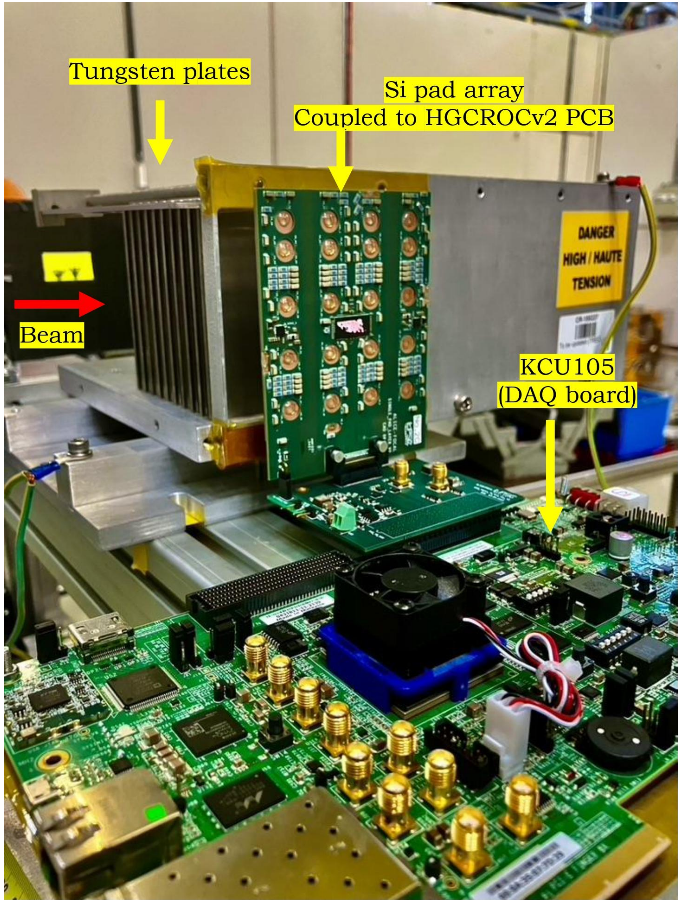

- W plates ~ 1 radiation length, placed behind the detector
- Si pad array coupled with HGCROCv2 PCB
- PCB connected to KCU105 board via interface board

Species	Energy in GeV
Pion (negative)	5, 10, 15
Electron	1, 2, 3, 4, 5

Radiation length	0, 1, 2, 3, 4, 5, 6, 8

Tests beam setup at PS CERN: Trigger Scheme

- Trigger: AND logic of Cherenkov and plastic scintillators
- Cherenkov not used for pion beam (>90% purity above 5 GeV pion)

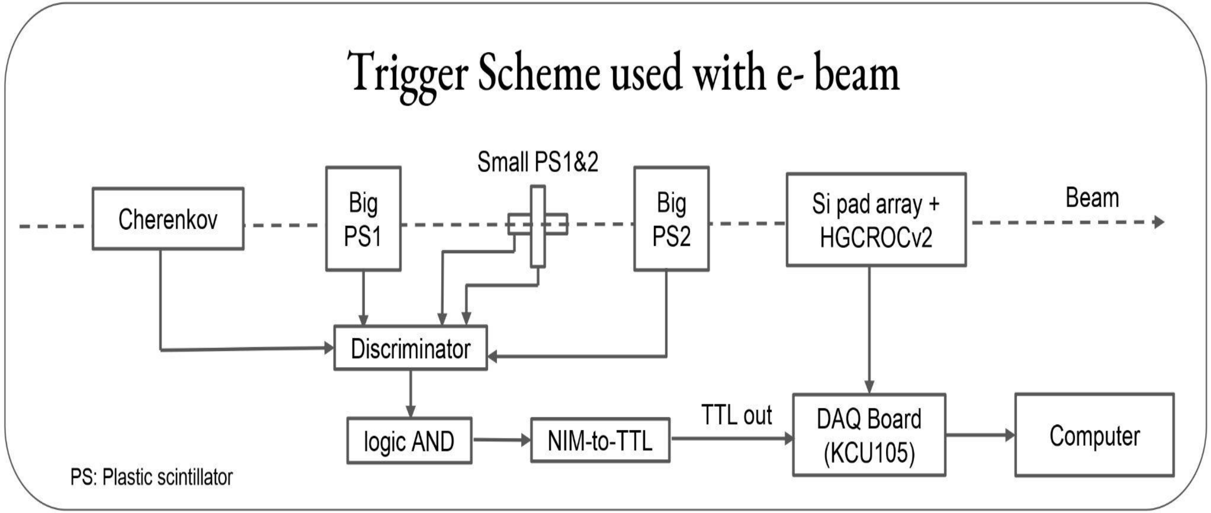

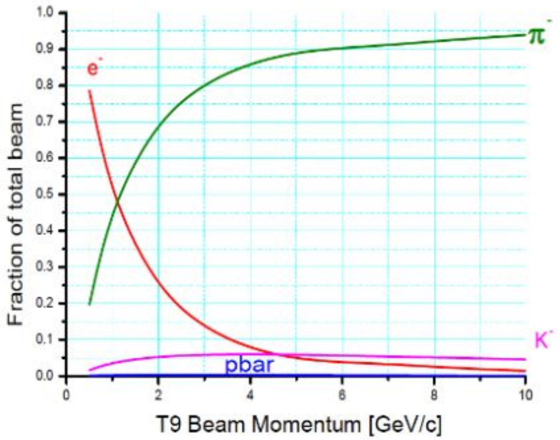

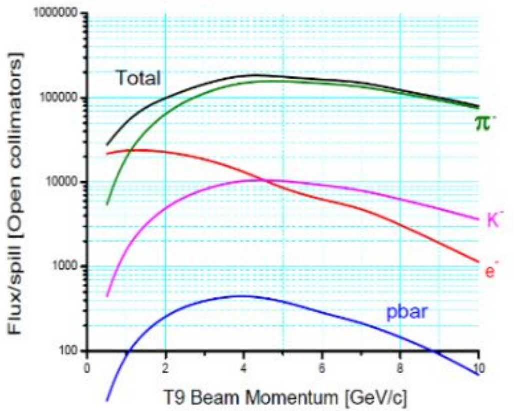

Geant4 test beam simulations

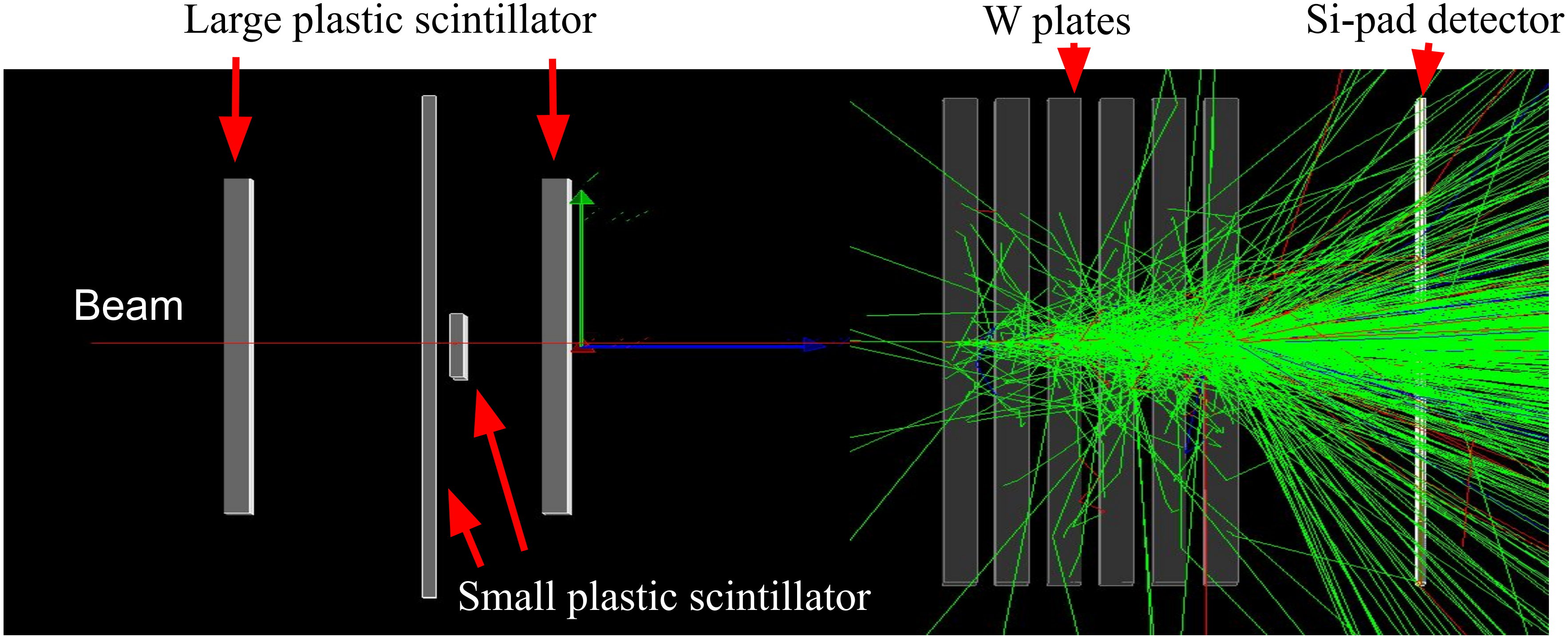

Particles	Energy (GeV)	W plates (~ $1X_0$)	Number of events
Pion (negative)	5, 10, 15	0	5000
Electron	1, 2, 3, 4, 5	0, 1, 2, 3, 4, 5, 6, 7, 8, 9, 10	10000

Typical noise distribution

Pedestal distribution of 4 channels in detector

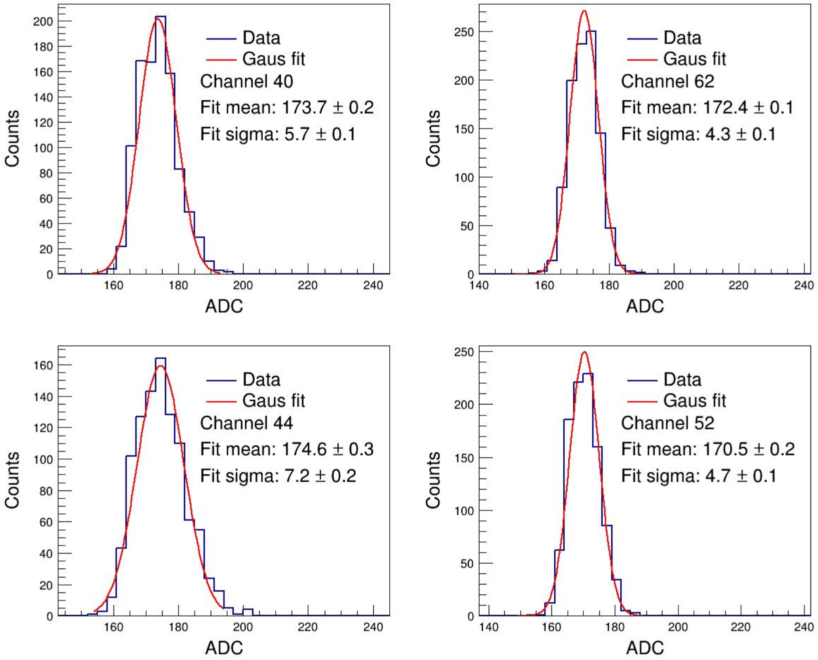

Pedestal follows gaussian distribution

Pedestal mean and rms value for all 72 channels

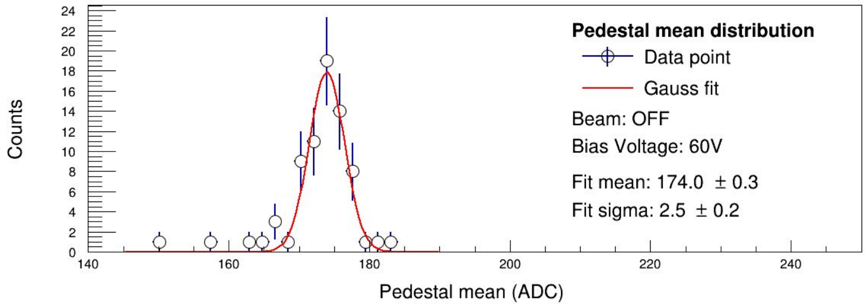

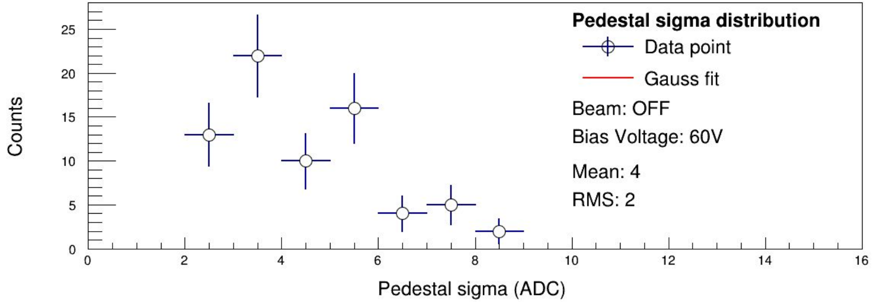

Mean pedestal ~ 174 ADC

Detector response to pion beam: MIP

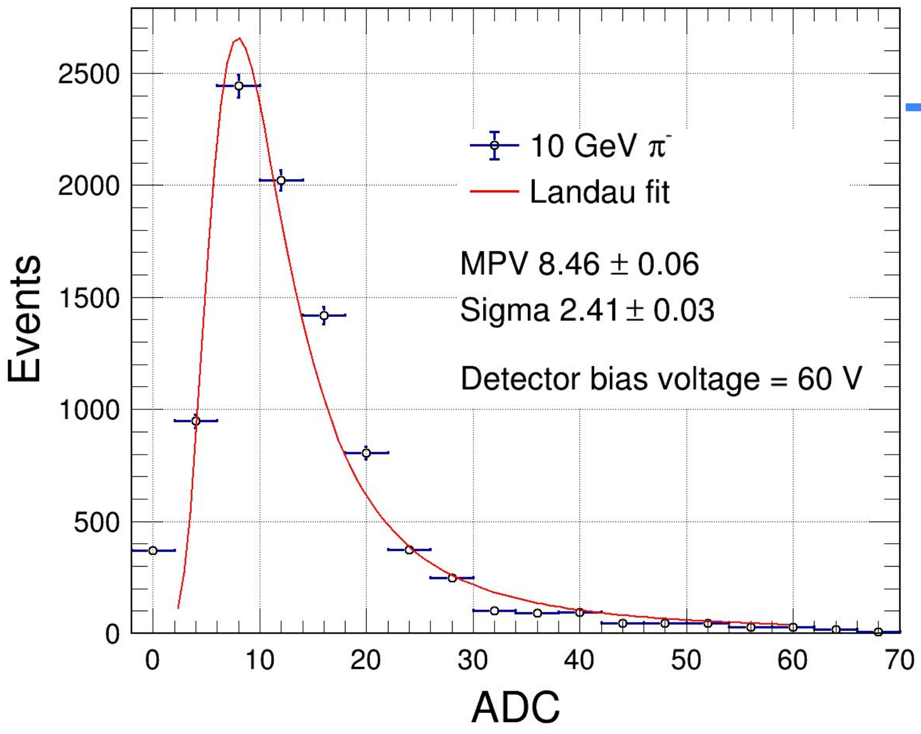

- 10 GeV π^- beam focused on one of the pad of detector
- Pedestal mean plus 3 sigma noise subtraction

A clear pion MIP signal is obtained, described by Landau function

Detector response to pion beam: MIP

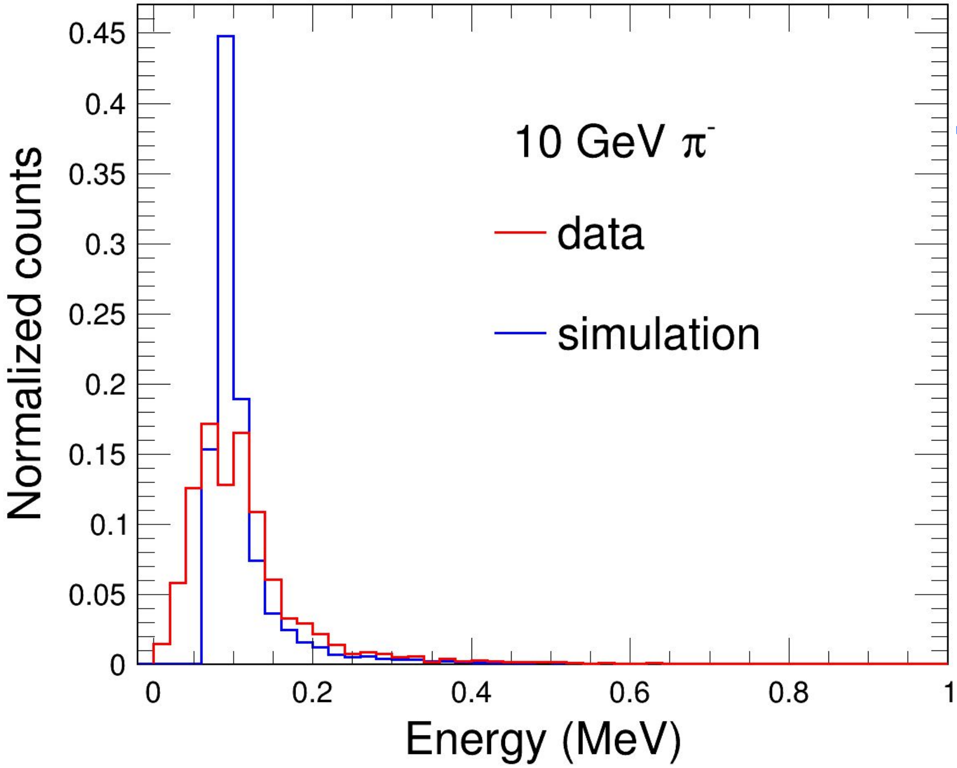

- Pion MIP comparison with Geant4 simulations
- Calibration of deposited energy from ADC to MeV (explained in upcoming slides)

The experimental data exhibits broader peaks than the simulated data, attributed to noise.

Detector response to pion beam: voltage scan

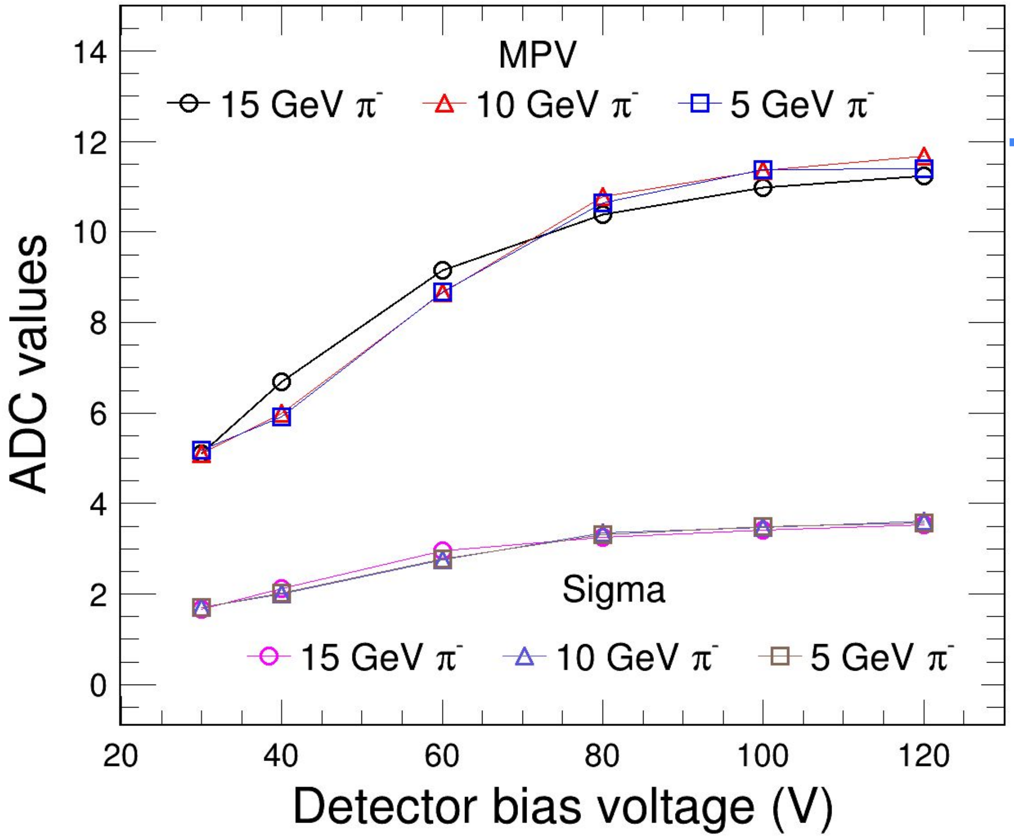

MPV and sigma of MIP pion is shown as a function of detector bias voltage

- MPV starts to saturate after bias voltage of 60 V.
- Standard deviation rises roughly by 1 ADC from 30 V to 120 V

Detector response to pion beam: Position scan

10 GeV pion beam focused on different channels during the position scan

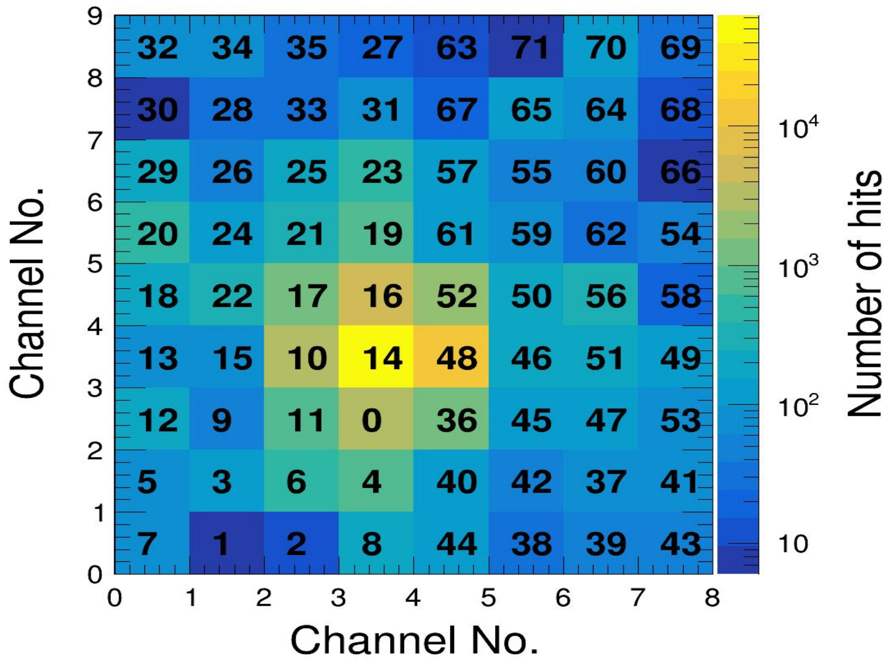

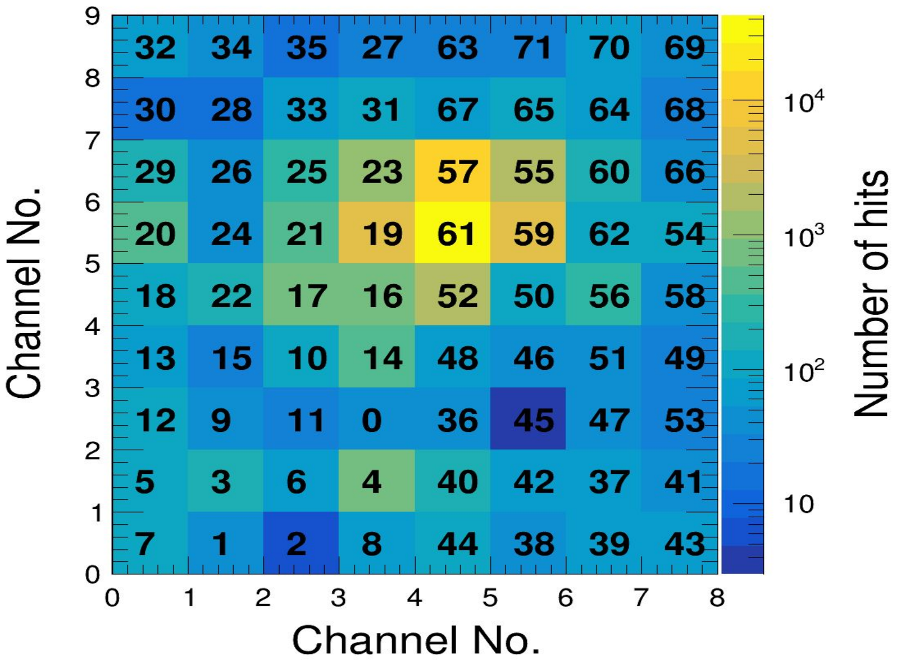

Position Scan: Detector gain correction

Before gain correction

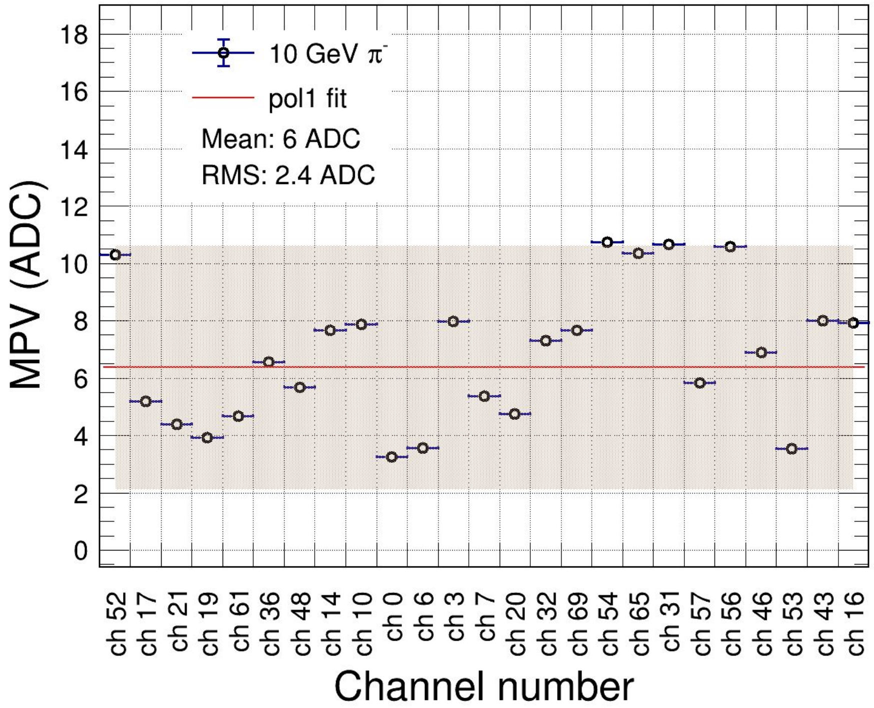

MPV RMS spread ~ 2 ADC values across the channels

After gain correction

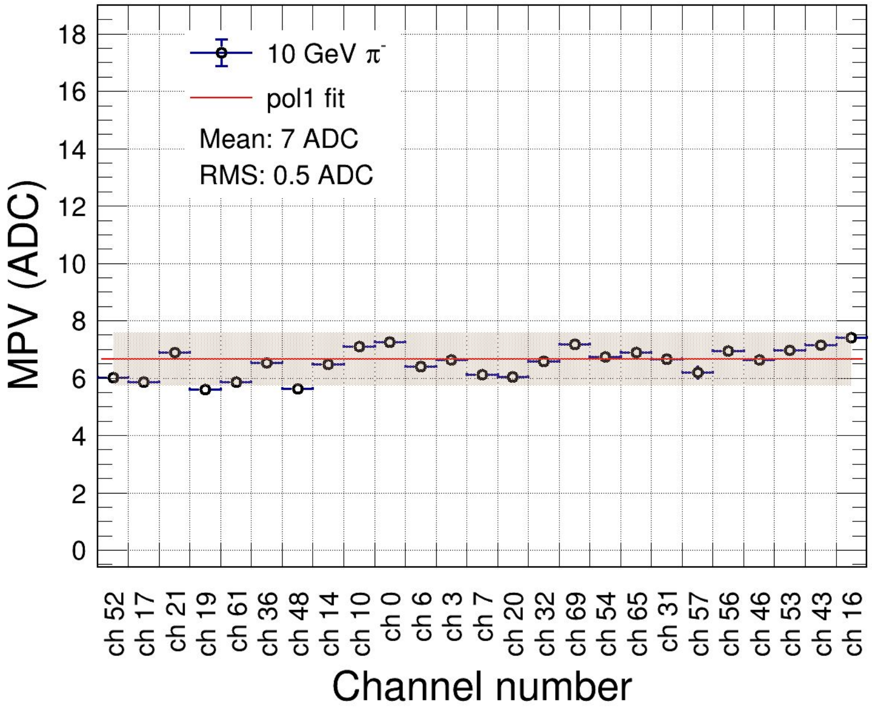

RMS Spread reduced significantly

Detector response to e^- beam: MIP

Data taken without any absorber plate before detector

Electron MIP

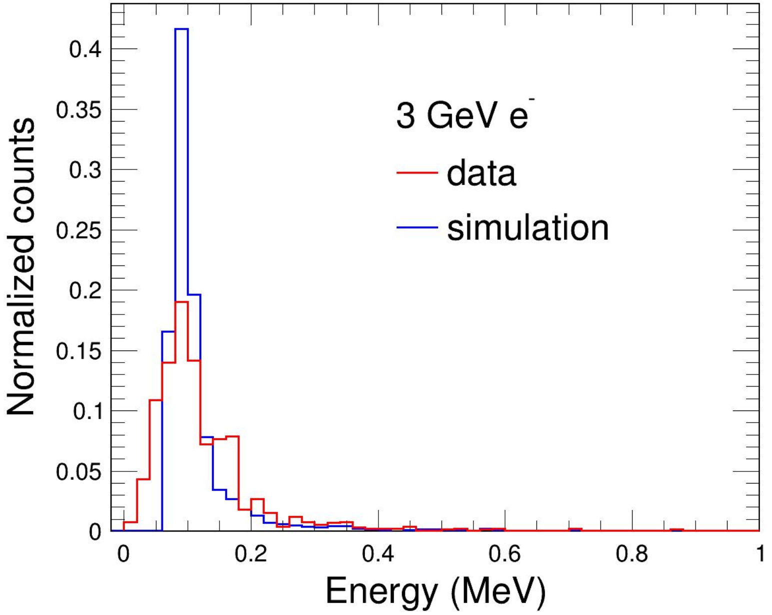

Pion MIP

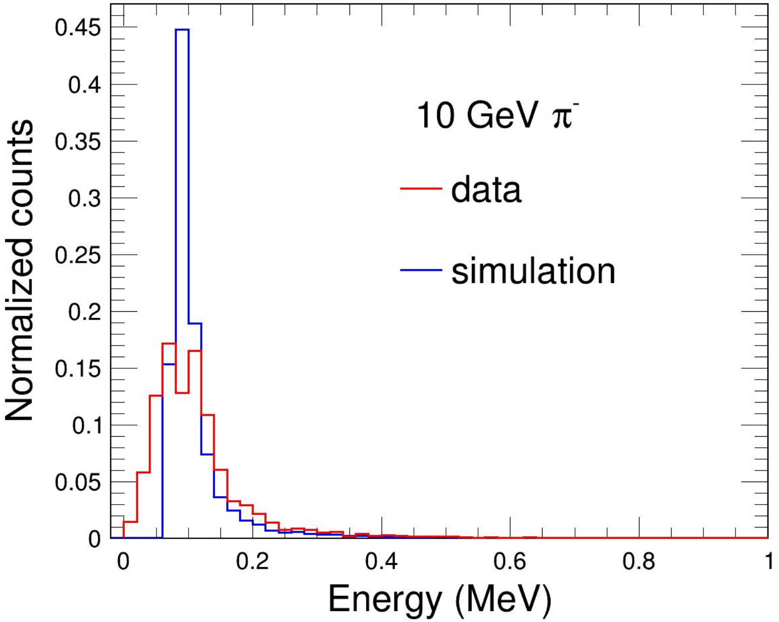

Both electron and pion mip from data has broader peaks than simulations due to noise

Electromagnetic cascades

A high energy electron or photon, incident on a thick absorber initiates an electromagnetic cascade through bremsstrahlung and pair production

Longitudinal shower development scales with radiation length

Electrons eventually fall beneath critical energy and lose further energy through dissipation and ionization

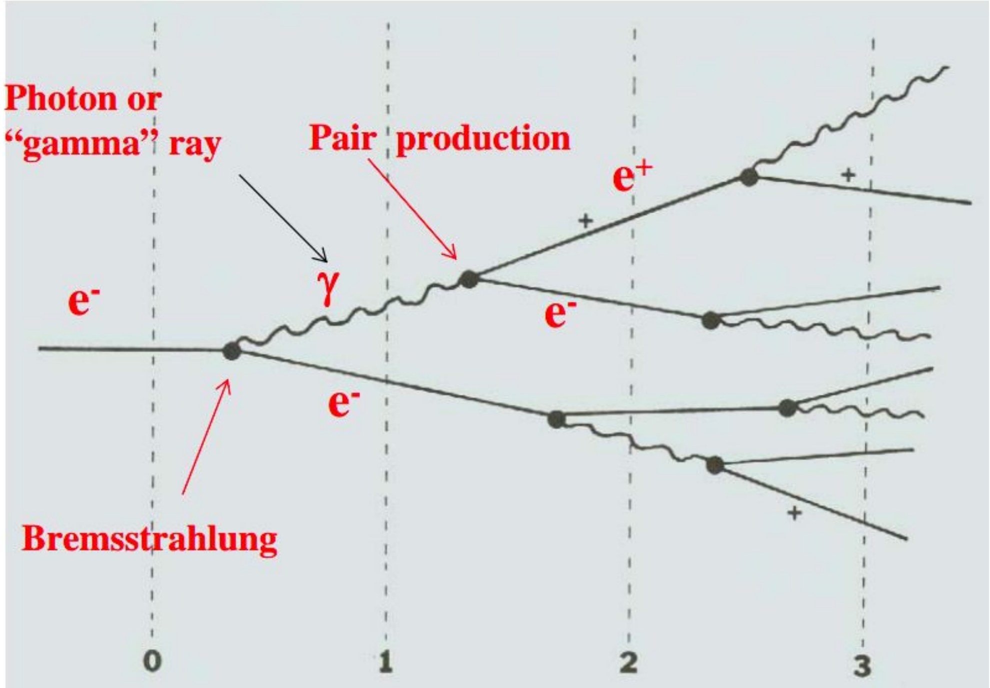

Radiation length

Detector response to e^- beam: Hit map

2 radiation lengths

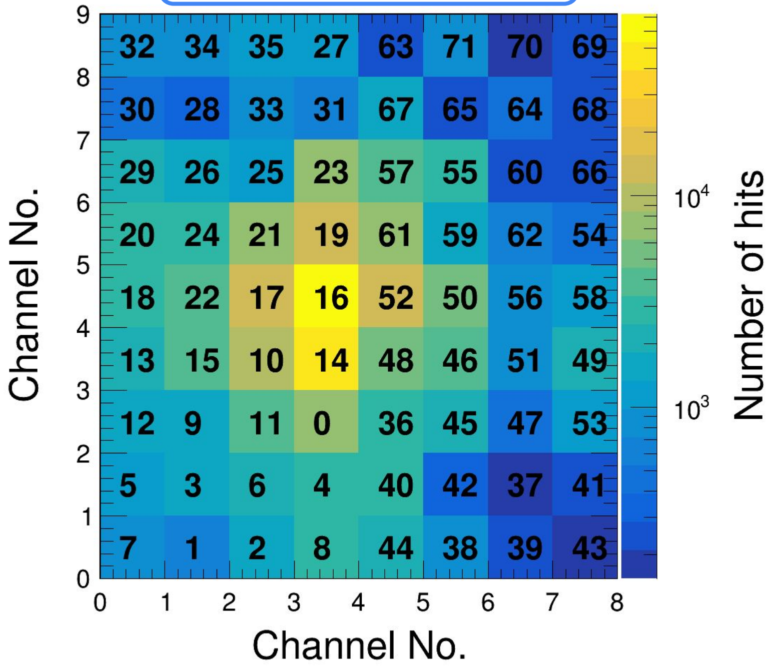

6 radiation lengths

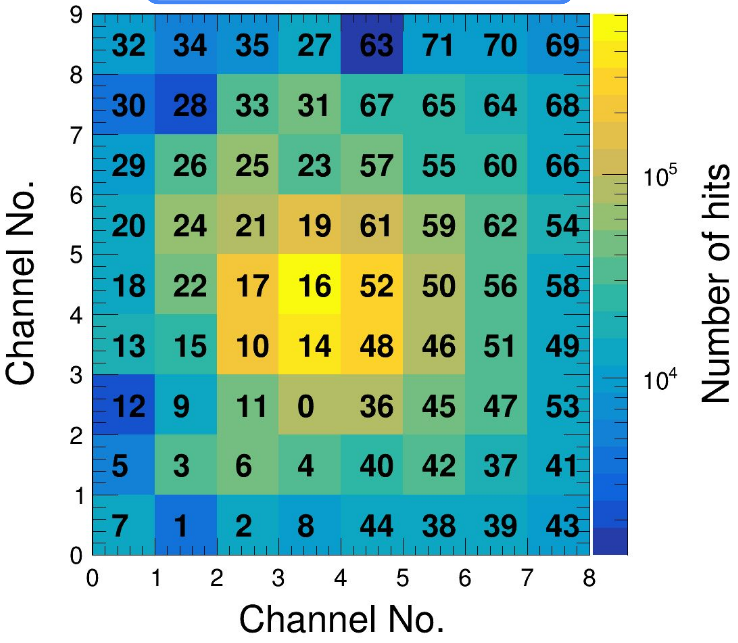

Electron-positron cascade is relatively narrow at 2 X_0 than 6 X_0

Detector response to e^- beam: Clustering algorithm

The algorithm focuses on identifying clusters of pads that are adjacent or connected to each other on the silicon detector

Before clustering

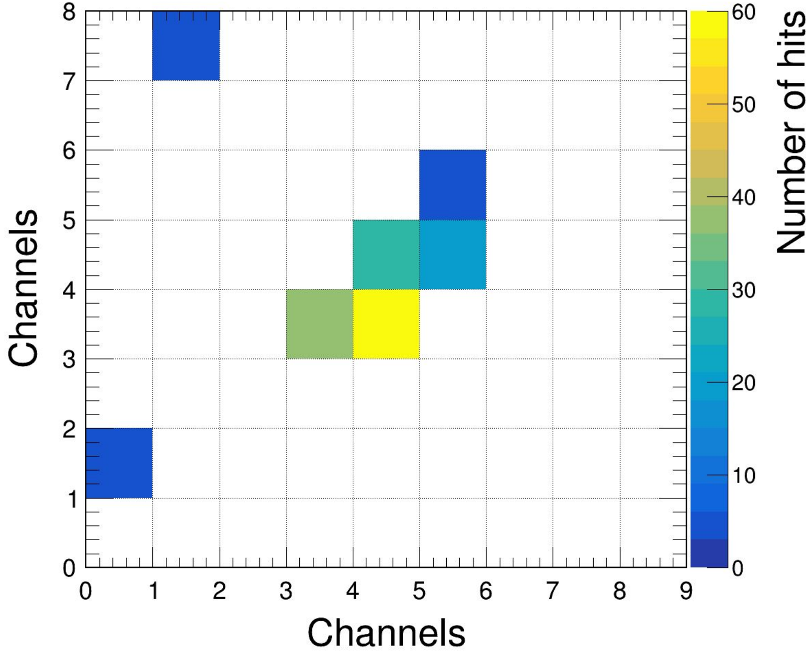

After clustering

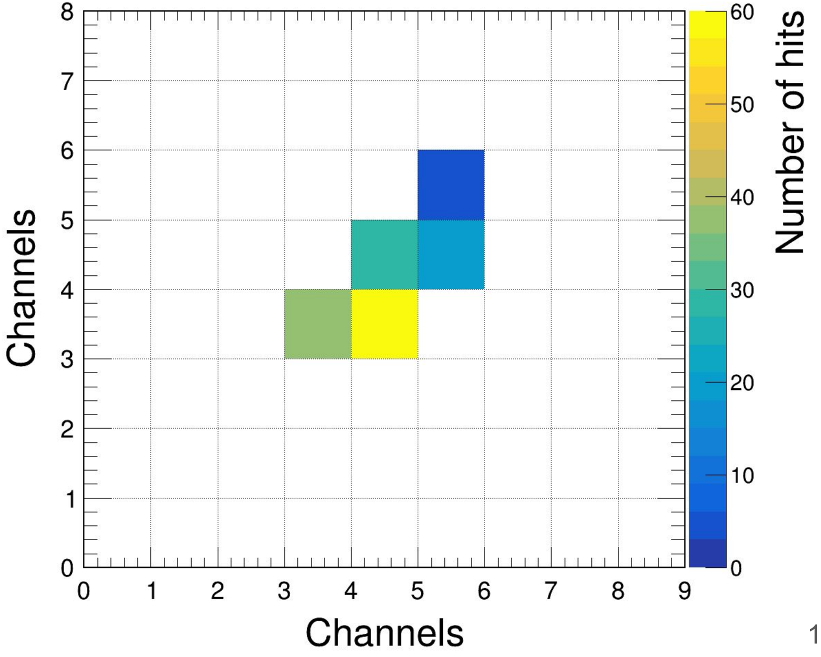

Detector response to e^- beam: Cluster ADC distribution

- Energy deposited by electrons (ADC) across 3 and 5 radiation lengths
- Clustering algorithm used to sum the energy across the pads in cluster

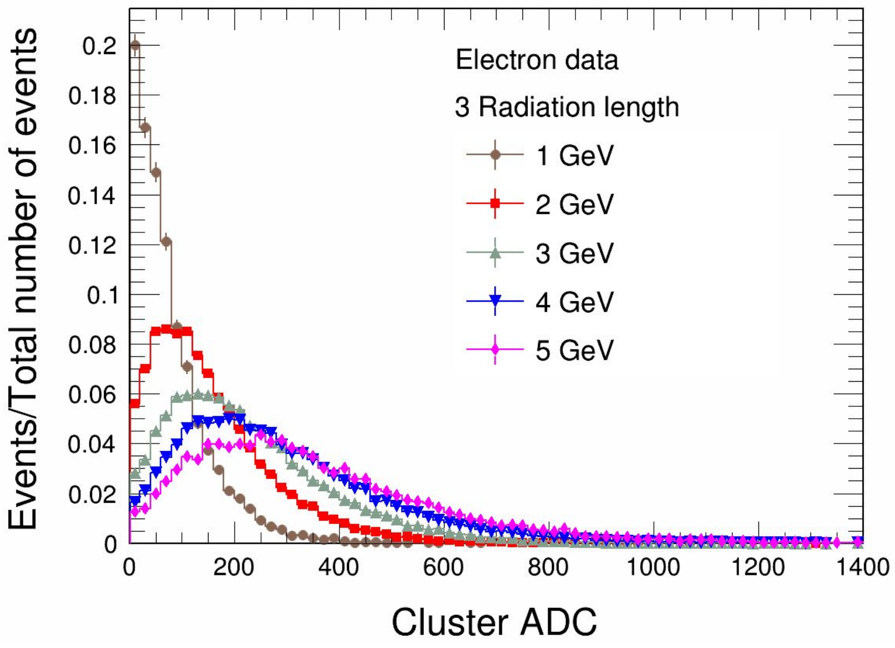

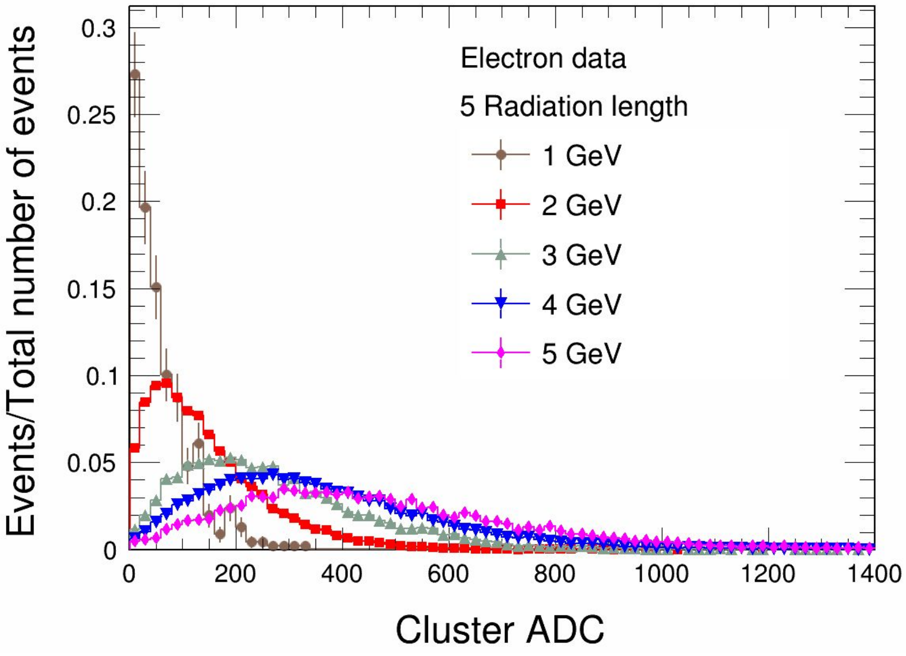

Energy deposition increases with increased electron energy

Detector response to e^- beam: Energy calibration

Linear trend is observed between the deposited energy in data (ADC) and simulations (MeV)

Energy deposition increases with increase in electron energy

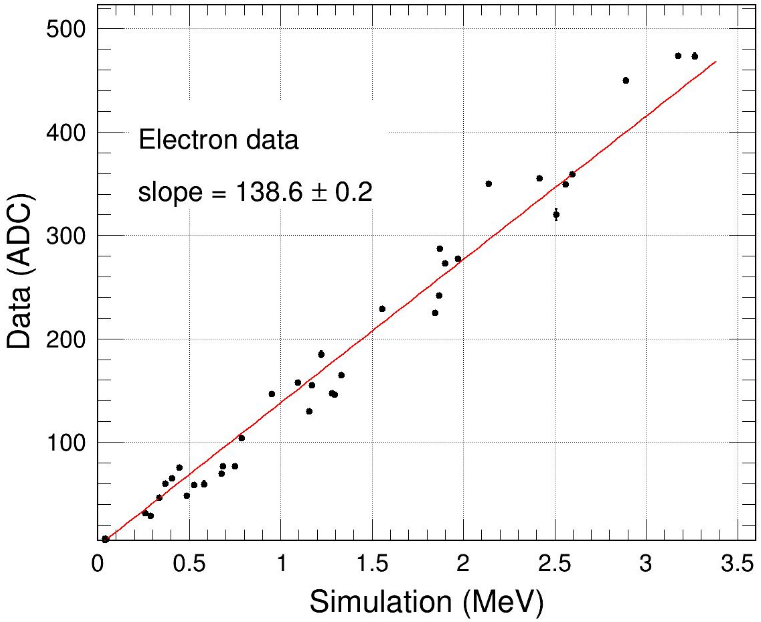

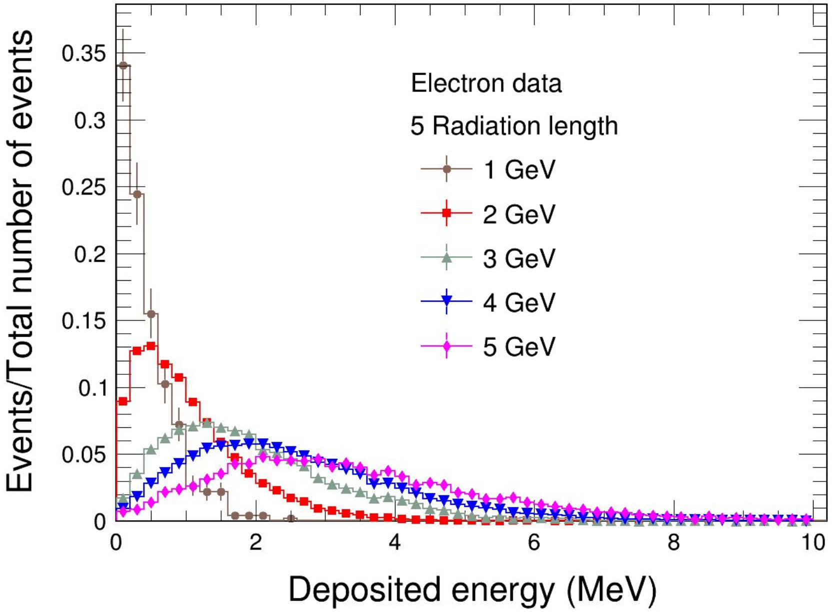

Detector response to e^- beam: Longitudinal shower profile

Higher energy particles push "shower maximum" deeper into the material (radiation length)

Mean cluster size represents the transverse dimension of electromagnetic showers

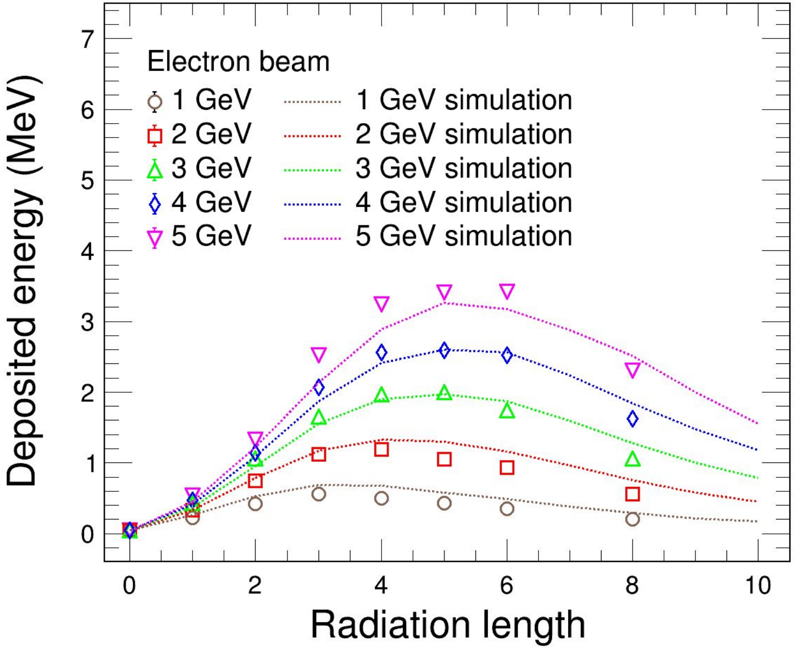

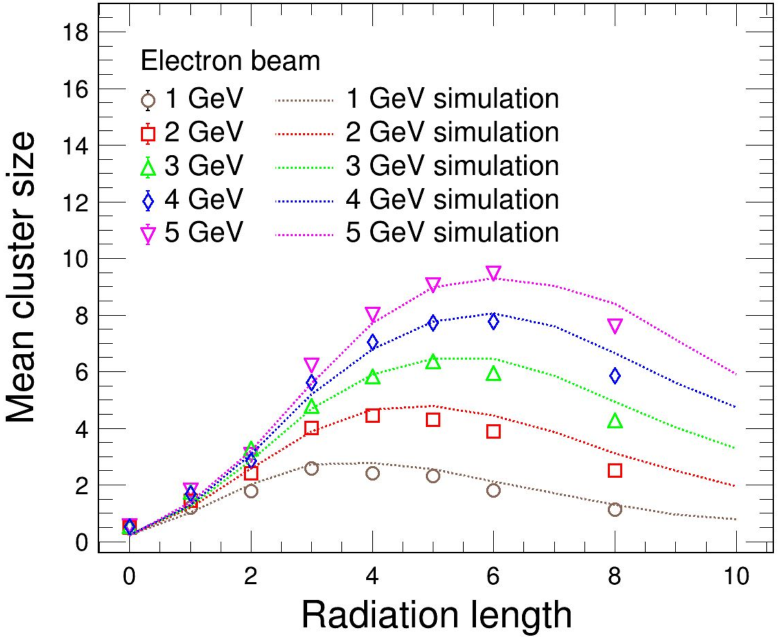

Detector response to e^- beam: Transverse energy profile

What causes transverse spread ?

- Finite opening angle between the e^-e^+ pair.
- Multiple scattering between electrons.

- 90 % of the total energy deposited, remains within 1 molar radius

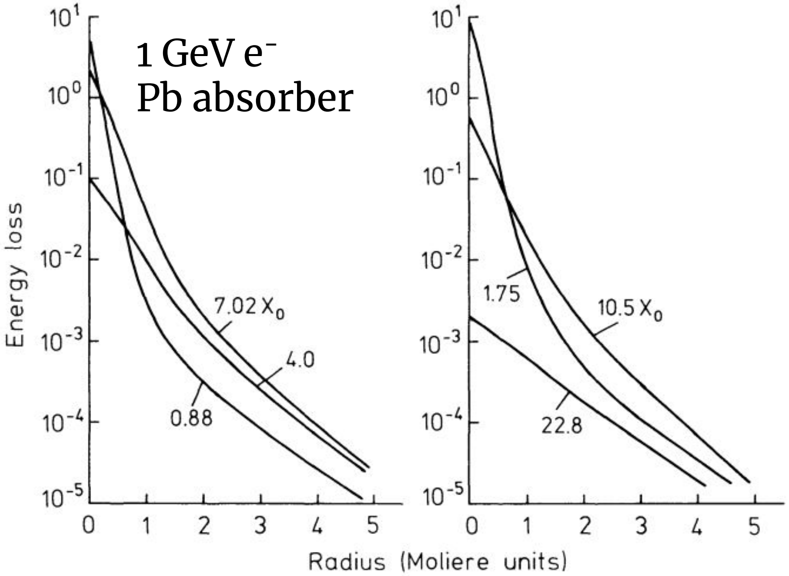

Leo, William R. *Techniques for nuclear and particle physics experiments.* Springer Science & Business Media, 2012.

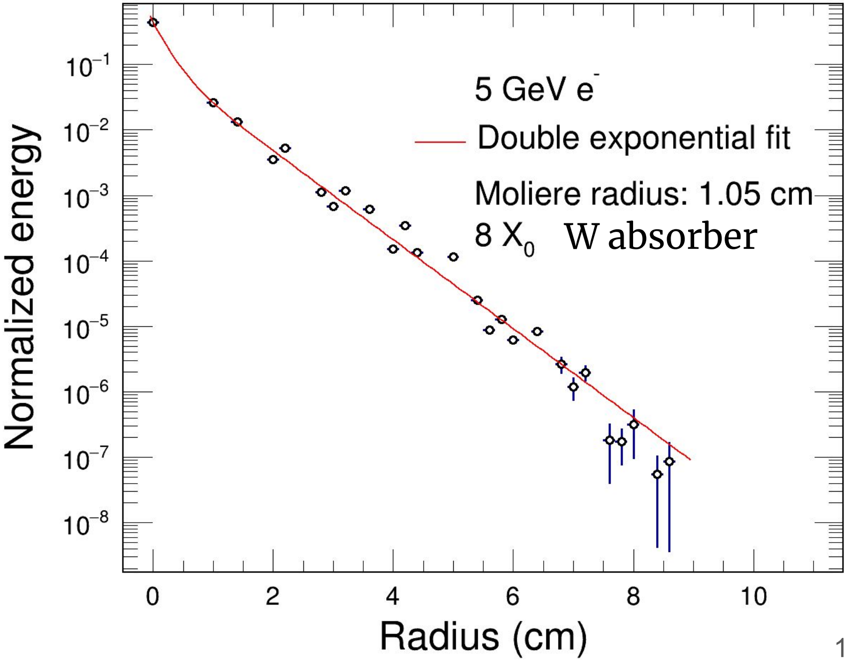

Detector response to e^- beam: Transverse energy profile

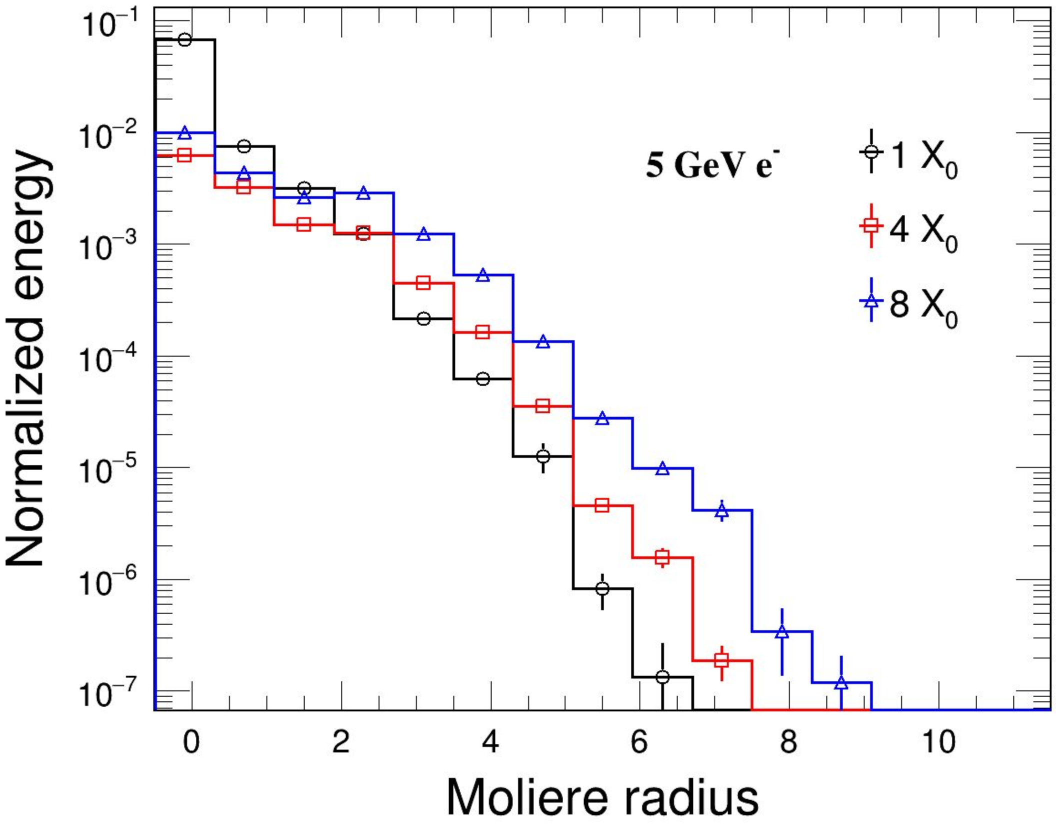

Distance from shower axis scaled with molar radius

- Cascade remains relatively narrow in the first radiation length
- The lateral shower profile becomes wider as we move to higher radiation length

Summary

- Clear MIP peak observed for 5 GeV, 10 GeV, and 15 GeV π^- beams at various positions on the Si pad array.
- Detector bias voltage scan using the pion beam determined the operating voltage.
- Gain correction performed to achieve uniform gain across all channels of the detector.
- Energy calibration is done to convert the deposited energy from ADC to MeV.
- Longitudinal shower profile for 1 GeV to 5 GeV electron showers with 0 to 8 tungsten plates is generated which is in agreement with the Geant4 simulations.
- Calculation of molar radius using the transverse shower profile of electrons

Acknowledgement

I would like to thank Bharat Electronics Limited (BEL), Bangalore, for the design and fabrication of the pad array detector and ALICE FoCal collaboration for their support throughout the test beam. Furthermore, I extend my thanks to the T9 area incharge for their assistance and support during the test beam.

Backup slides

Mean energy loss: Bethe-Bloch

$$\frac{-dE}{dx} = K z^2 \frac{Z}{A} \frac{1}{\beta^2} \left[\frac{1}{2} \ln \frac{2 m_e c^2 \beta^2 \gamma^2 T_{max}}{I^2} - \beta^2 - \frac{\delta(\beta\gamma)}{2} \right]$$

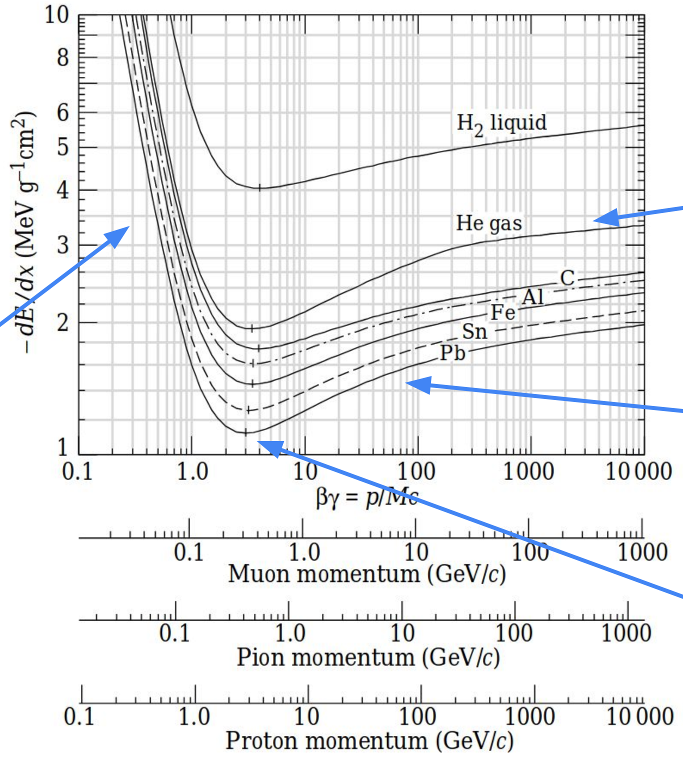

Kinematical term
<dE/dx> ~ 1/β²

Fermi plateau

Relativistic rise
<dE/dx> ~ ln(β²γ²)

Minimum Ionizing Particles (MIPs)
βγ ≈ 2-4

Typical noise distribution: 72 Channels

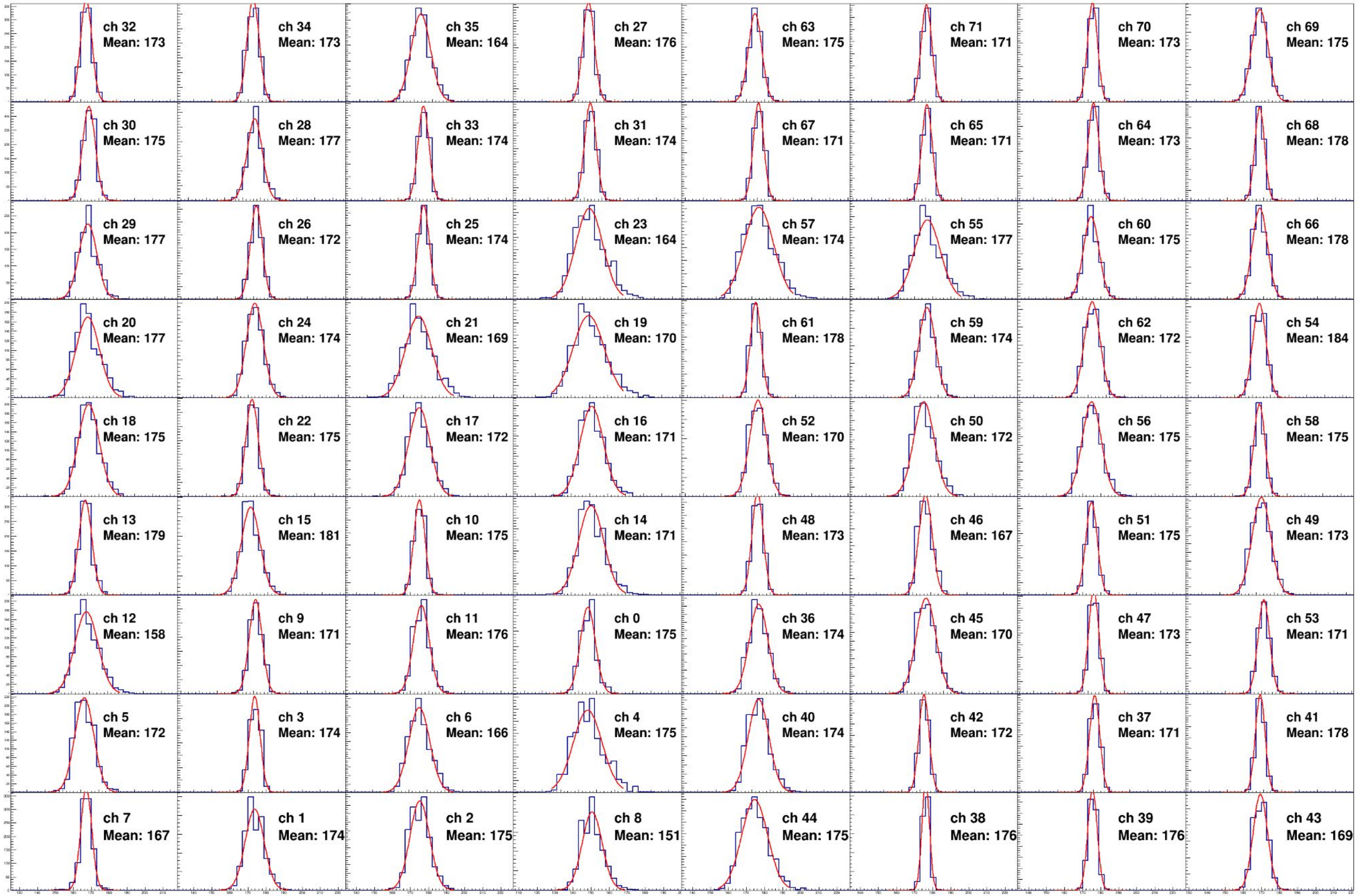

- Pedestal distribution for all 72 channels
- Pedestal fit with gaussian function

Typical noise distribution: Multiple background data

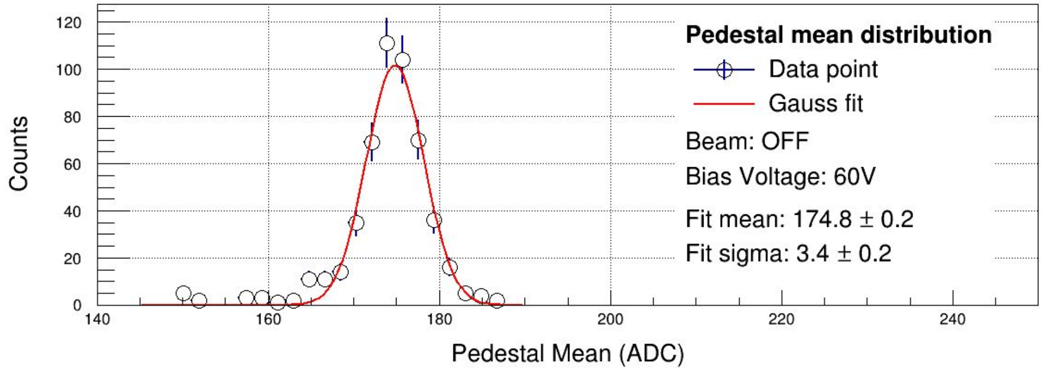

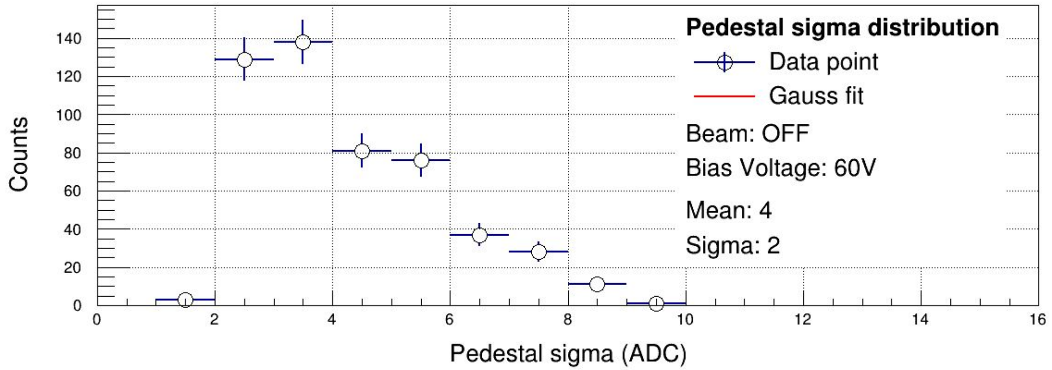

Pedestal mean distribution of 72 channels of 7 different datasets.

Typical noise distribution: Detector OFF

- Pedestal distribution of 4 channels in detector
- Pedestal is fit with gaussian function

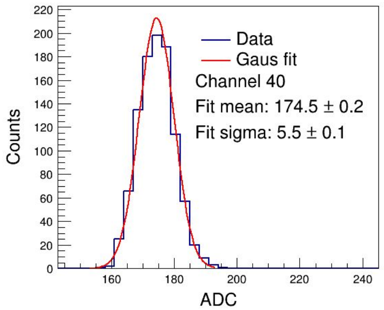

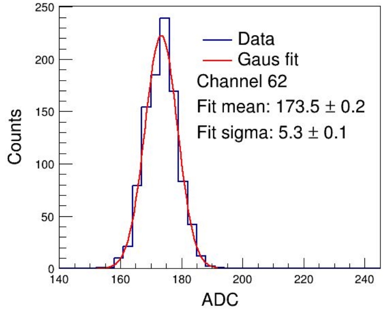

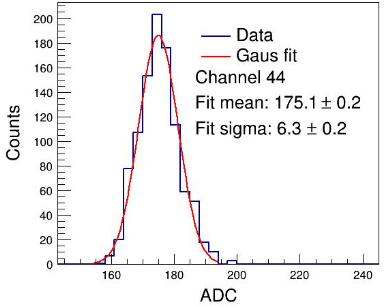

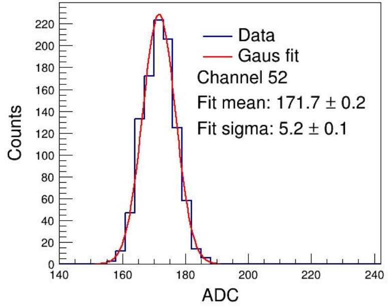

- Pedestal mean value for 72 channels
- Bias voltage: 60V
- Mean pedestal ~ 173 ADC

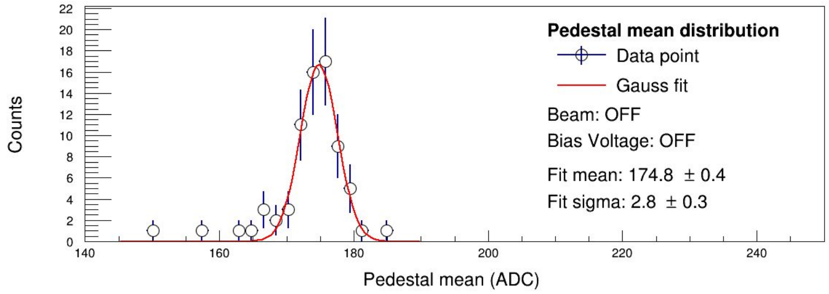

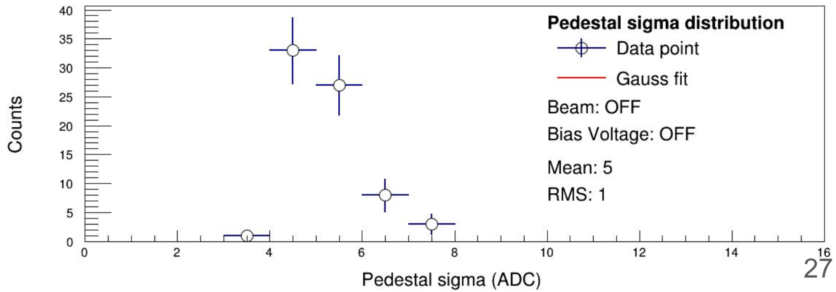

Typical noise distribution: Multiple background data

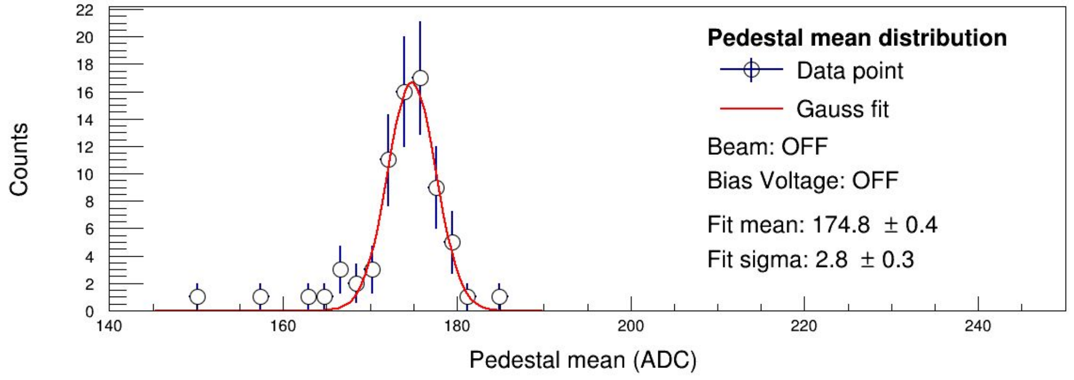

Pedestal mean distribution of 72 channels of 6 different datasets.

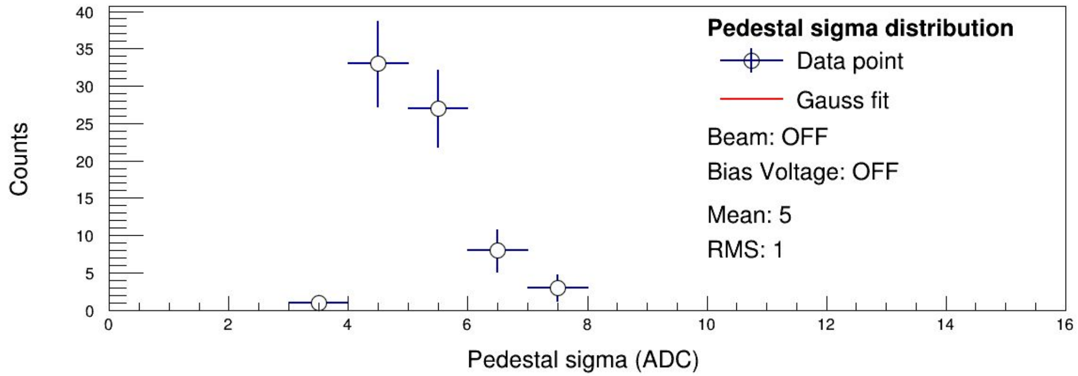

Same pedestal mean value is observed with bias voltage on and off

Detector operating voltage: CV plot

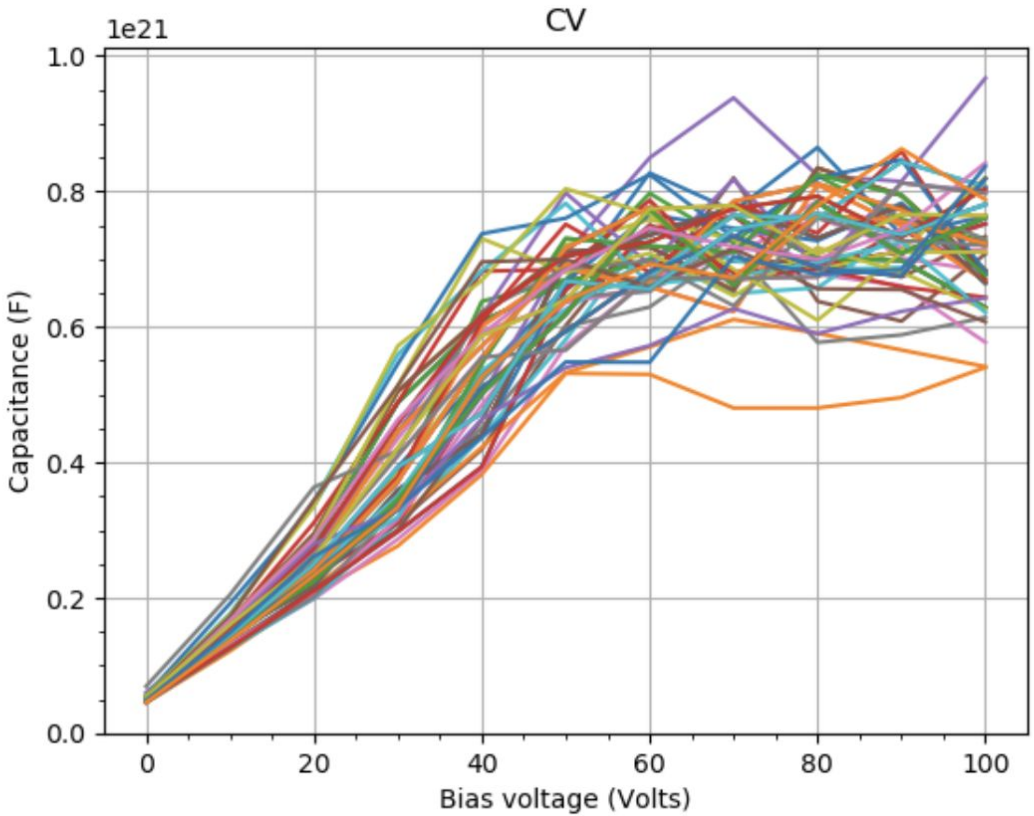

Capacitance vs voltage measurements across the 72 pads in the detector

Pion MIP: Position scan data (after calibration)

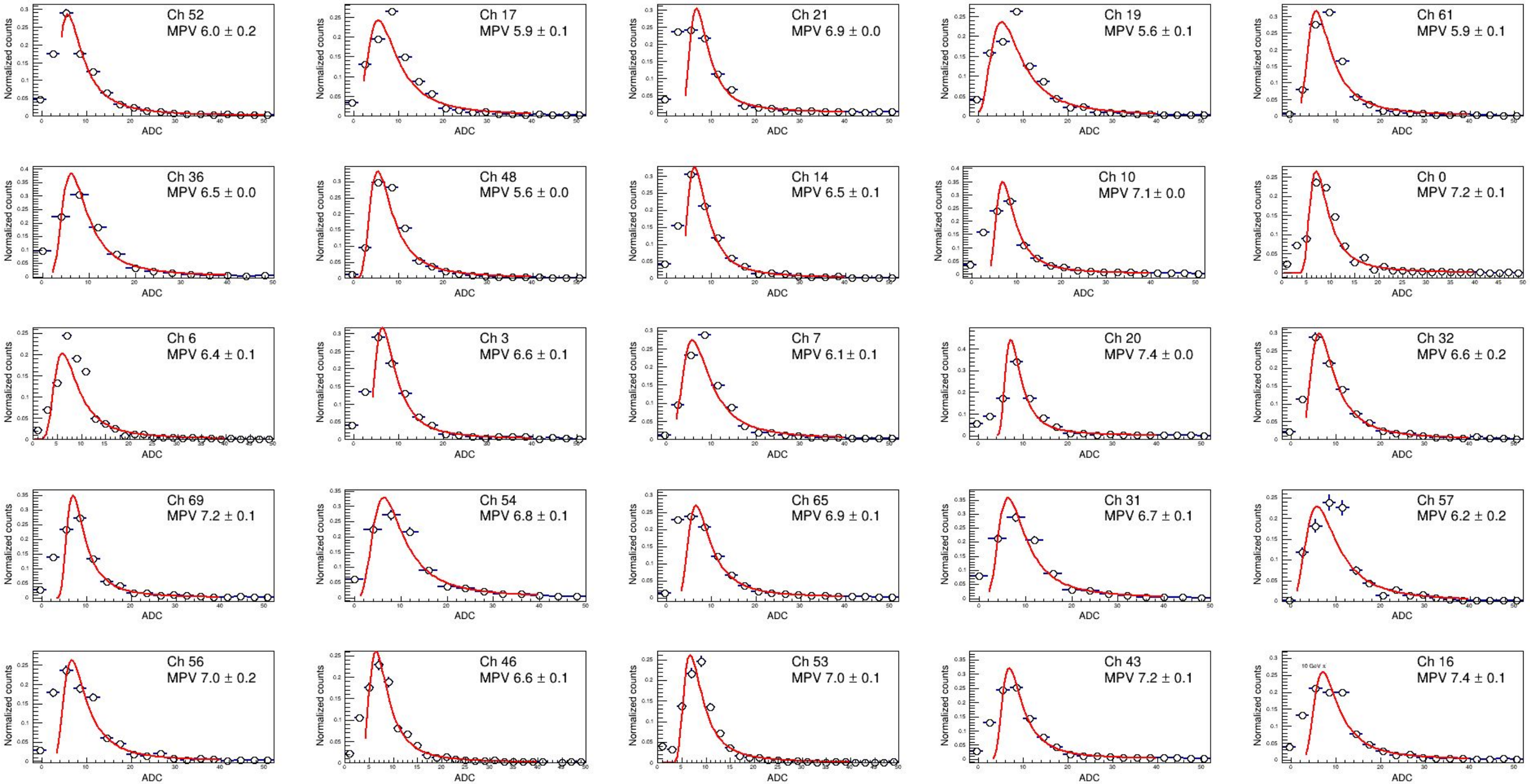

- 10 GeV π^-
- Landau fit

Detector response to e^- beam: Cluster ADC distribution

- Energy deposited by electrons in MeV values across 5 radiation lengths

Data

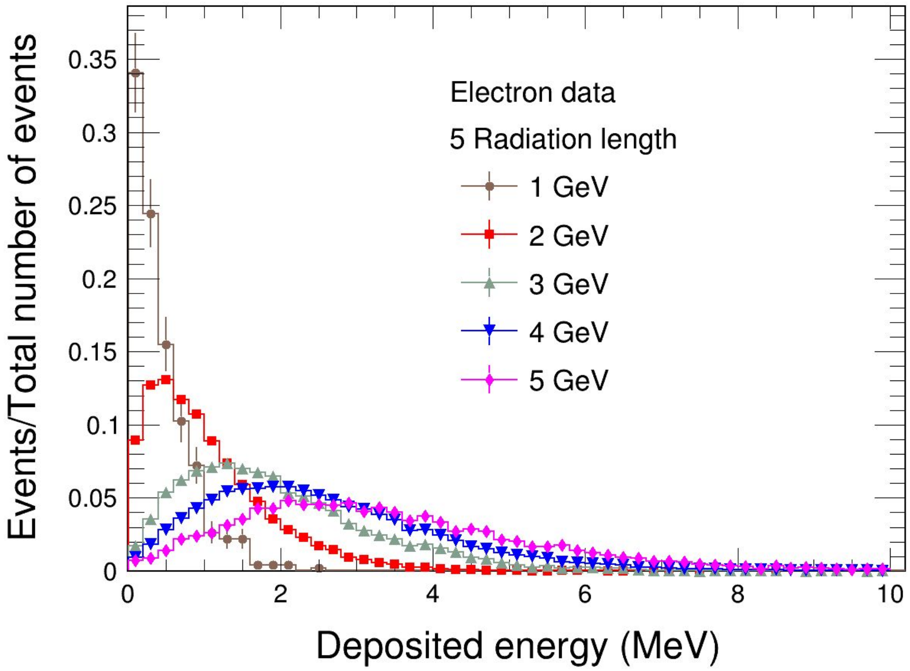

Simulations

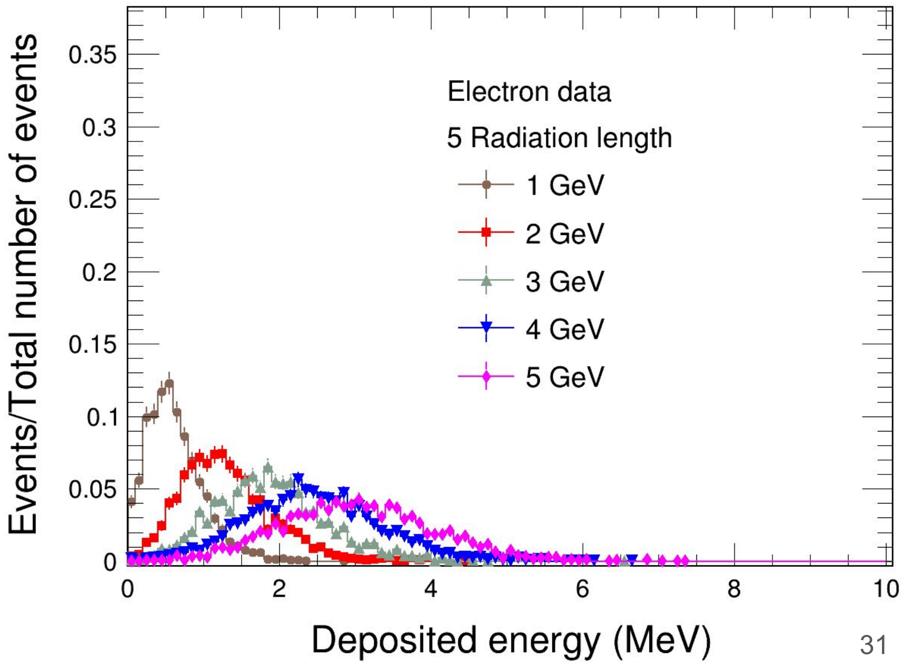

Percentage deviation of data with simulations: Shower profile

Energy (GeV) \ X_0	0	1	2	3	4	5	6	8
1	1.6	12.7	19.4	18.6	26.3	26.0	28.0	28.3
2	2.4	0.1	4.5	4.2	10.6	18.6	19.1	26.0
3	9.4	17.1	11.3	6.1	3.7	1.6	6.6	17
4	3.7	15.3	3.9	10.7	5.9	0.2	1.3	11.9
5	23.8	21.3	8.9	18.0	12.3	4.6	7.7	7.9